Biogenic Silver Nanoparticles for Acid Red Dye Remediation in Aquatic Systems: Structural Characterization and Ecotoxicological Evaluation

Dr. Vandana Pandey

Assistant Professor, Department of Botany, Shri AKPG College, Bulanala, Varanasi, Uttar Pradesh, India
pandeyvandanadr@gmail.com

ABSTRACT

The increasing discharge of textile dye effluents into aquatic ecosystems poses serious environmental and ecological challenges, necessitating the development of sustainable and efficient remediation strategies. In the present study, biogenic silver nanoparticles (AgNPs) were synthesized using natural pond water as a green reducing and stabilizing medium and evaluated for their potential in Acid Red dye remediation under semi-natural conditions. The biosynthesized AgNPs were characterized using X-ray diffraction (XRD), field emission scanning electron microscopy (FE-SEM), and energy-dispersive X-ray spectroscopy (EDX). XRD analysis confirmed the formation of crystalline face-centered cubic silver with prominent reflections corresponding to (111), (200), (220), and (311) planes (JCPDS card No. 04-0783), while FE-SEM imaging revealed predominantly spherical nanoparticles with an estimated size range of 150–300 nm. Average crystallite size, estimated via the Debye–Scherrer equation, ranged from 15 to 35 nm, consistent with nanoscale silver formation. EDX spectroscopy confirmed elemental silver as the dominant signal, accompanied by trace chlorine and nitrogen peaks attributable to biogenic capping residues.

The remediation efficiency and ecological impact were assessed by monitoring total protein content—measured by the Lowry method at 660 nm—as a biochemical indicator of microbial metabolic activity across control, dye-treated, nanoparticle-treated, and combined exposure systems over a four-day incubation period. A consistent, time-dependent decline in protein concentration was observed in all treatment groups, with comparatively greater inhibition recorded in the combined dye + AgNP system (OD_{4th} = 0.23), suggesting synergistic enhancement of dye transformation coupled with augmented biological stress. Statistical analysis using F-test ($p = 0.1092$), independent t-test ($p = 0.3210$), and Wilcoxon Signed-Rank test ($p = 0.50$) indicated no significant inter-group differences at $\alpha = 0.05$; however, Pearson's correlation analysis demonstrated a strong negative relationship between incubation time and protein levels ($r = -0.95$ to -0.99), indicating progressive and reproducible metabolic suppression across treatments.

necessity for careful dosage optimization and environmental risk assessment to mitigate possible ecotoxicological impacts. This study contributes to advancing green nanotechnology approaches for sustainable wastewater management.

Keywords: Green synthesis, Silver Nanoparticles, Nano-Bioremediation, Acid Red Dye, Aquatic Ecotoxicology, X-Ray Diffraction (XRD), Textile Wastewater Treatment, Protein Biomarker Analysis

Introduction

The rapid expansion of industrial activities, urbanization, and population growth has exerted unprecedented pressure on global freshwater resources, resulting in the continuous discharge of untreated or partially treated wastewater into natural aquatic systems. Industrial effluents frequently contain hazardous contaminants such as heavy metals, synthetic dyes, pharmaceuticals, endocrine-disrupting compounds (EDCs), and persistent organic pollutants (POPs), which accumulate in water bodies and disrupt ecological balance (Rehman, 2020; Crini & Lichtfouse, 2019). These contaminants not only deteriorate water quality but also pose serious risks to aquatic organisms and human health through bioaccumulation and biomagnification across trophic levels **(Gupta & Singhal, 2020; Fu & Wang, 2011).**

Among these pollutants, synthetic textile dyes represent a significant environmental challenge due to their complex aromatic structures, high chemical stability, and resistance to biodegradation. Dyes such as Acid Red are widely used in textile processing and are frequently detected in industrial effluents at concentrations ranging from 10 to 200 mg/L. Even at sub-lethal concentrations, these dyes impart intense coloration to water bodies, reduce light penetration, inhibit photosynthetic activity, and may produce toxic or carcinogenic intermediates upon partial degradation **(Tasi-Lu & Liu, 2001).** Conventional wastewater treatment technologies, including coagulation–flocculation, activated sludge processes, membrane filtration, and adsorption techniques, are frequently limited by high operational costs, sludge generation, incomplete degradation, and reduced efficiency in removing recalcitrant dye molecules **(Crini & Lichtfouse, 2019; Gupta & Singhal, 2020).** Consequently, there is a pressing need for innovative and sustainable remediation strategies capable of addressing dye contamination effectively.

Nanotechnology has emerged as a promising alternative for environmental remediation due to the unique physicochemical properties of nanomaterials, including high surface area-to-volume ratio, enhanced catalytic reactivity, and tunable surface functionalities **(Qu et al., 2013).** Metal nanoparticles, particularly silver nanoparticles (AgNPs), have demonstrated considerable potential in pollutant adsorption, redox transformation, and photocatalytic

degradation of organic contaminants. In addition to their well-established antimicrobial properties, AgNPs exhibit strong interactions with complex azo dye molecules through mechanisms including electron transfer, reactive oxygen species (ROS) generation, and surface plasmon resonance-mediated photocatalysis **(Veronica et al., 2023).** Previous studies have reported significant dye decolorization efficiencies using biologically synthesized AgNPs, including 85.8% decolorization of Congo Red by AgNPs produced from *Aspergillus niger* broth within 24 hours **(Nithya et al., 2019).**

However, conventional physicochemical synthesis methods for nanoparticles—such as chemical reduction, hydrothermal techniques, and sol–gel processes—often require toxic reagents and generate hazardous by-products, thereby conflicting with principles of green chemistry (Iravani, 2011). To overcome these limitations, green or biogenic synthesis approaches have gained substantial attention. Biosynthesis utilizing plant extracts, algae, fungi, bacteria, or natural water systems offers an eco-friendly, cost-effective, and scalable alternative in which naturally occurring biomolecules—including polyphenols, flavonoids, proteins, and polysaccharides—act simultaneously as reducing and stabilizing agents (Ahmad et al., 2010; Song & Kim, 2009). Such biomolecule-assisted synthesis enhances nanoparticle colloidal stability and may influence crystallographic orientation and surface reactivity **(Pal et al., 2007).**

Despite their promising remediation efficiency, the environmental deployment of nanoparticles raises concerns regarding ecotoxicological impacts. Nanoparticles may undergo aggregation, dissolution, and physicochemical transformation in aquatic environments, altering their bioavailability and interaction potential with non-target organisms **(Cristafulli-Bunsu, 2016).** Silver nanoparticles, in particular, have been reported to exert concentration-dependent toxicity on aquatic microorganisms and microalgae such as *Chlamydomonas* and marine phytoplankton species **(Granbardella et al., 2015; Huang et al., 2016; Seelam et al., 2017, 2018; Dedman et al., 2015).** Suppression of cyanobacterial biomass and microbial protein synthesis has also been documented following AgNP exposure **(Dulman et al., 2020).** Therefore, while nano-bioremediation offers enhanced pollutant removal efficiency, its ecological safety must be carefully evaluated **(Kaul & Sharma, 2022; Bundschuh, 2016).**

Recent advances in nanobioremediation emphasize the integration of biological systems with nanomaterials to improve degradation efficiency while reducing secondary pollution **(Rathodur, 2021; Kaul & Sharma, 2022).** Natural aquatic matrices, such as pond water enriched with dissolved organic matter and diverse microbial consortia, represent a potentially sustainable yet underexplored medium for nanoparticle biosynthesis. The complex biochemical milieu of natural pond water—containing humic substances, extracellular polymeric substances, and a variety of microalgal metabolites—may collectively facilitate effective metal ion reduction and nanoparticle stabilization without requiring exogenous chemical inputs. However, limited studies have examined the dual functionality of such biosynthesized nanoparticles in semi-natural aquatic conditions, particularly with simultaneous assessment of remediation efficiency and ecological response indicators. In this context, the present study investigates the green synthesis of silver nanoparticles using natural pond water as a biogenic medium and evaluates their effectiveness in the remediation of Acid Red dye under controlled yet environmentally relevant conditions. Structural and morphological characterization of the synthesized nanoparticles was performed using X-ray diffraction (XRD), field emission scanning electron microscopy (FE-SEM), and energy-dispersive X-ray spectroscopy (EDX), following established characterization protocols **(Sarkar et al., 2010; Jemal Kero et al., 2017).** Furthermore, protein content was employed as a biochemical biomarker to assess microbial metabolic responses and potential ecotoxicological effects associated with dye and nanoparticle exposure. By integrating physicochemical characterization with biological response assessment, this study aims to contribute to the advancement of sustainable green nanotechnology approaches for dye-contaminated wastewater treatment while addressing associated environmental risk considerations.

Materials And Methods

2.1 Study Site and Sample Collection

A natural pond water body showing maximum phytoplankton biomass density—assessed by visual turbidity and microscopic examination—was selected as the biological matrix for nanoparticle synthesis and experimental exposure. The site was chosen by random spatial sampling to minimize selection bias. Approximately 5 L of surface water was collected in acid-washed polypropylene containers, transported on ice, and processed within 6 hours of collection to preserve the integrity of dissolved organics and microbial populations.

2.2 Dye Preparation

Acid Red (Acid Violet) dye—a sulfonated azo dye commonly detected in textile processing effluents—was selected for this investigation. A primary stock solution was prepared by dissolving
1.0 g of the dye in 100 mL of double-distilled deionized water (DDW) under constant magnetic stirring for 30 minutes. Defined volumes of this stock were added to individual experimental flasks to achieve the targeted working concentrations required by each treatment group.

2.3 Biogenic Synthesis of Silver Nanoparticles (AgNPs)

Silver nitrate ($AgNO_3$; analytical grade, Merck) served as the metal precursor. A 30 mM stock solution was prepared in DDW and diluted to a working concentration of 15 mM within each experimental flask. Biogenic synthesis was

initiated by combining the $AgNO_3$ solution with natural pond water (1:1 v/v ratio) under ambient temperature (25 ± 2 °C) in dark incubation to preclude photoreduction artefacts. Nanoparticle formation was monitored visually and confirmed by the characteristic color transition described in the Results section.

2.4 Experimental Design

Four treatment groups were established in triplicate to evaluate individual and combined effects:

- Control (C): Untreated natural pond water
- C + AgNP: Pond water supplemented with biosynthesized AgNPs
- C + Dye: Pond water with Acid Red dye
- C + AgNP + Dye: Pond water with both AgNPs and Acid Red dye

All flasks were incubated under controlled laboratory conditions (25 ± 2 °C, 12 h light/12 h dark photoperiod). Sampling was conducted at Day 0, Day 2, Day 3, and Day 4 for biochemical analysis.

2.5 Characterization of AgNPs

X-ray Diffraction (XRD) analysis was performed using a Bruker D8 Advance diffractometer with Cu Kα radiation ($\lambda = 0.15406$ nm) at 40 kV and 40 mA over the 2θ range 20–80°. Diffractograms were compared against JCPDS reference card No. 04-0783 for metallic silver. Mean crystallite size was calculated using the Debye–Scherrer equation: $D = K\lambda / (\beta \cos\theta)$, where $K = 0.94$, β is the FWHM in radians, and θ is the Bragg angle. Morphological analysis was conducted by Field Emission Scanning Electron Microscopy (FE-SEM; ZEISS SIGMA VP, 5 kV) after gold sputter-coating. Elemental composition was confirmed by Energy-Dispersive X-ray (EDX) spectroscopy coupled to the FE-SEM system.

2.6 Protein Quantification

Total soluble protein content was quantified using the Lowry method (Lowry et al., 1951) with bovine serum albumin (BSA) as the standard. Aliquots (1 mL) were collected from each treatment flask, centrifuged at 3,000 rpm for 10 min, and the supernatant was used for assay. Optical density was measured at 660 nm using a UV-Vis spectrophotometer (Shimadzu UV-1800). All measurements were performed in triplicate and expressed as mean OD ± SD.

2.7 Statistical Analysis

Data were analyzed using Microsoft Excel and SPSS v23.0. Parametric tests (one-way ANOVA with F-test, independent samples t-test) and the non-parametric Wilcoxon Signed-Rank test were employed to assess inter-group differences. Pearson's correlation coefficient (r) was computed to evaluate temporal trends. A significance level of $\alpha = 0.05$ was maintained throughout.

Results

3.1 Visual Confirmation and Biosynthesis of AgNPs

Nanoparticle formation was evident within 24 hours of incubating $AgNO_3$ solution with pond water. A progressive color transition from pale brown → dark brown → black was observed (Fig. 1), attributable to the well-characterized surface plasmon resonance (SPR) phenomenon of silver nanoparticles in the 400–450 nm optical window (Jemal Kero et al., 2017). The persistent black coloration over subsequent days indicated colloidal stability conferred by biogenic organic capping agents present in the pond water matrix.

Fig. 1: *(A) Natural Pond water biosample selected for AgNP synthesis; (B) Color transition in reaction flask*

showing progressive change from pale brown to dark black indicating AgNP formation; (C) Experimental setup showing control and treatment flasks (C, C+AgNP, C+Dye, C+AgNP+Dye)

3.2 X-Ray Diffraction Characterization

The crystalline structure of biosynthesized AgNPs was confirmed by XRD analysis. The experimental diffractogram (Fig. 2A) displayed sharp, well-resolved peaks at 2θ values of 38.1°, 44.3°, 64.5°, and 77.5°, indexed respectively to the (111), (200), (220), and (311) crystallographic planes of face-centered cubic (fcc) metallic silver. These reflections align precisely with the JCPDS reference pattern No. 04-0783 (Fig. 2C), confirming phase-pure fcc silver without

detectable oxide or salt impurities. A comparative diffractogram recorded in the presence of Acid Red dye (Fig. 2B) revealed marginally sharper and more intense peaks, suggesting that dye molecules may have influenced crystallization kinetics by acting as supplementary capping agents, promoting more ordered crystal growth along the (111) orientation.

The (111) plane consistently exhibited the highest relative intensity in both experimental and reference spectra, consistent with preferential growth along the thermodynamically stable low-surface-energy (111) facet in biogenically synthesized silver nanoparticles (Pal et al., 2007). Minor additional reflections in the experimental pattern are attributed to residual organic material from the biogenic synthesis route, a feature commonly observed in green synthesis literature (Song & Kim, 2009). The Debye–Scherrer equation applied to the (111) peak yielded an average crystallite size of 15–35 nm, consistent with nanoscale silver formation. Slight peak broadening indicated the sub-50 nm regime and reflected the diversity of crystallite sizes present in the biogenic preparation.

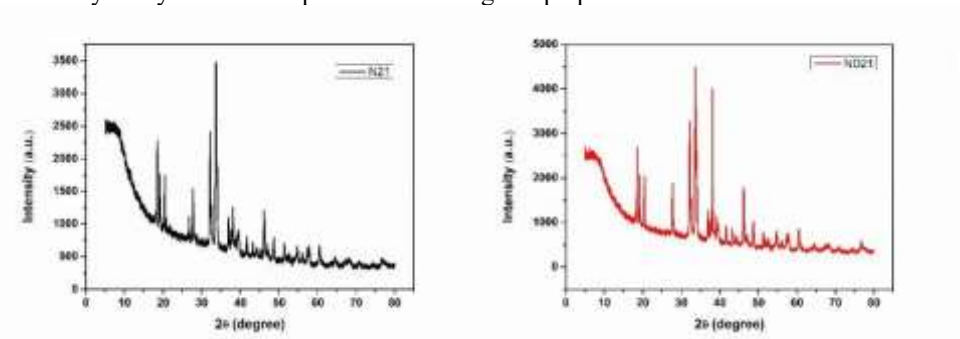

Fig. 2: *XRD diffraction patterns of biosynthesized AgNPs: (A) in the presence of Acid Red dye; (B) without dye; (C) JCPDS reference pattern No. 04-0783 for face-centered cubic metallic silver. Indexed Miller planes (111), (200), (220), and (311) confirm phase-pure fcc silver*

3.3 FE-SEM and EDX Analysis

Field Emission Scanning Electron Microscopy confirmed the predominantly spherical morphology of the biosynthesized AgNPs (Fig. 3A). Particle size distribution estimated from FE-SEM micrographs ranged from 150 to 300 nm, representing the hydrodynamic diameter inclusive of biogenic organic capping layers—larger than XRD-derived crystallite sizes, as expected for aggregated or organically coated nanoparticle assemblies (Chugh et al., 2021). Some clustering was observable, consistent with the aggregation behavior typical of biogenically synthesized nanoparticles in aqueous suspension without additional surfactant stabilization.

Energy-Dispersive X-ray spectroscopy (Fig. 3B) confirmed elemental silver as the dominant signal, with the characteristic Ag Lα peak at approximately 3.0 keV. Trace signals for chlorine (Cl) and nitrogen (N) were detected, attributable to chloride ions and nitrogen-containing biomolecules from the pond water matrix incorporated into the biogenic capping layer. These organic residues are consistent with protein and polysaccharide adsorption onto the nanoparticle surface, which confers colloidal stability and contributes to biocompatibility of the nanoparticles in aquatic media (Sarkar et al., 2010).

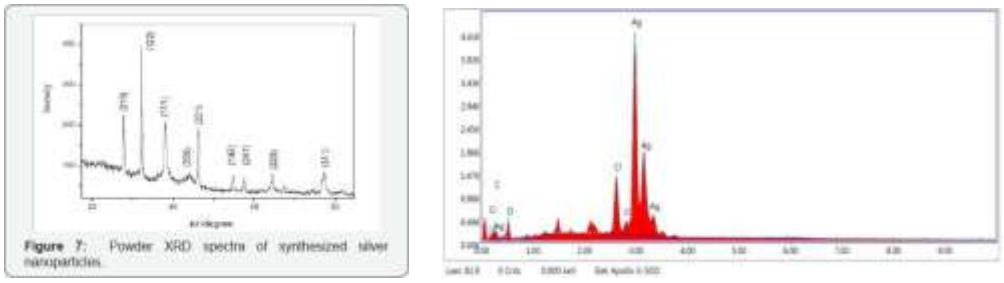

Fig. 3: *(A) FE-SEM micrograph of biosynthesized AgNPs showing predominantly spherical morphology with particle size range 150–300 nm; (B) EDX spectrum confirming dominant elemental silver (Ag Lα, ~3.0 keV) with trace signals for Cl and N derived from biogenic capping residues in pond water matrix*

3.4 Effect on Microbial Protein Content

Protein content, measured as OD at 660 nm using the Lowry method, served as a quantitative indicator of microbial metabolic activity and biological stress across all treatment groups. All groups commenced with an identical baseline OD of 0.72, and exhibited a consistent, progressive decline over the four-day incubation period (Table 1; Fig. 4).

The control group (C) showed a moderate protein decline (OD: 0.72 → 0.34), reflecting the natural senescence of pond water microbial communities under controlled laboratory conditions. The C + AgNP group demonstrated a more pronounced decrease (OD: 0.72 → 0.26), consistent with prior reports of AgNP-mediated suppression of

cyanobacterial biomass and protein synthesis (Dulman et al., 2020). The C + Dye group similarly exhibited enhanced protein reduction (OD: 0.72 → 0.27), corroborating the inhibitory effects of azo dyes on aquatic microbial communities (Tasi-Lu & Liu, 2001). Critically, the combined C + AgNP + Dye treatment produced the greatest protein inhibition (OD: 0.72 → 0.23), demonstrating a synergistic interaction between dye toxicity and nanoparticle stress, which may be mediated by amplified reactive oxygen species generation at the AgNP–dye interface (Modi et al., 2015).

Table 1: Protein content (OD at 660 nm) of pond water across treatment groups over four days (values represent Mean ± SD, n = 3)

Day	Control (C)	C + AgNP	C + Dye	C + AgNP + Dye
0	0.72 ± 0.02	0.72 ± 0.02	0.72 ± 0.02	0.72 ± 0.02
2nd	0.43 ± 0.02	0.40 ± 0.02	0.43 ± 0.02	0.43 ± 0.02
3rd	0.36 ± 0.02	0.285 ± 0.02	0.295 ± 0.02	0.255 ± 0.02
4th	0.34 ± 0.02	0.26 ± 0.02	0.27 ± 0.02	0.23 ± 0.02

C = Control; AgNP = Biosynthesized Silver Nanoparticles; Dye = Acid Red dye

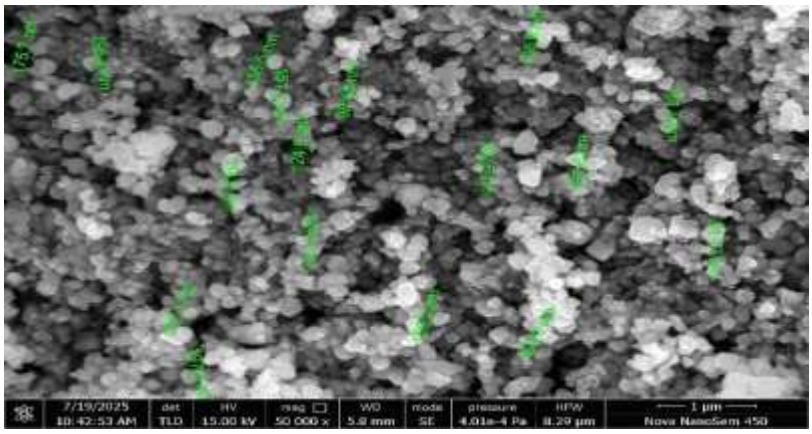

Fig. 4: *Temporal variation in protein content (OD at 660 nm) across treatment groups—Control (C), C + AgNP, C + Dye, and C + AgNP + Dye—over four days of incubation. All groups show progressive protein decline; the combined AgNP + Dye group exhibits the greatest inhibition, indicative of synergistic stress effects*

3.5 Statistical Analysis

Statistical evaluation of protein data using one-way ANOVA (F-test: p = 0.1092), independent samples t-test (p = 0.3210), and the non-parametric Wilcoxon Signed-Rank test (p = 0.50) indicated no statistically significant inter-group differences at α = 0.05. This absence of significance is attributable to the limited replication (n = 3), inherent biological variability of natural pond water systems, and the relatively short four-day experimental window. Notwithstanding, Pearson's correlation analysis revealed a strong negative temporal correlation between incubation time and protein content across all treatment groups (r = −0.95 to −0.99), confirming a consistent, reproducible trend of progressive metabolic decline. These results underscore that biological significance and statistical significance are not synonymous, and that effect-size interpretation is essential in ecotoxicological studies with small experimental replication.

Discussion

The present investigation provides integrated evidence for the biogenic synthesis of silver nanoparticles using natural pond water as an ecologically sourced reducing and capping medium, and their application in Acid Red dye remediation under semi-natural aquatic conditions. The findings are discussed in the context of green nanotechnology, nano-bioremediation efficiency, and aquatic ecotoxicology.

The characteristic color progression from pale brown to black observed during synthesis reflects the well-documented surface plasmon resonance of silver nanoparticles, driven by the collective oscillation of conduction electrons at nanoparticle surfaces. The natural pond water matrix, enriched with dissolved organic matter, humic acids, extracellular polymeric substances, and diverse microbial metabolites, serves as an effective multi-component bioreducing system. This extends the established framework of algal- and microbial-mediated biosynthesis (Sarkar et al., 2010; Jemal Kero et al., 2017) to demonstrate that unmodified natural water can function as a cost-free, self-contained bioreactor without requiring organism isolation, extract preparation, or exogenous chemical agents.

XRD characterization confirmed phase-pure fcc metallic silver with preferential (111) orientation, consistent with the

thermodynamically favorable low surface energy configuration of this crystallographic face in green synthesis (Pal et al., 2007). The Debye–Scherrer-derived crystallite size of 15–35 nm places these particles firmly in the nano-regime. The discrepancy between XRD crystallite sizes and FE-SEM particle sizes (150–300 nm) reflects particle aggregation in aqueous suspension and the contribution of biogenic organic capping layers that are transparent to electron diffraction but visible under SEM imaging. This multi-crystalline particle architecture is characteristic of biogenic synthesis routes and has been consistently reported in the literature (Chugh et al., 2021; Dahnormane et al., 2017). The slightly enhanced peak intensity observed in dye + AgNP samples suggests that sulfonated azo dye molecules may act as secondary molecular templates or capping agents, modulating crystal growth and potentially enhancing surface reactivity.

The progressive, time-dependent suppression of microbial protein content across all treatment groups is consistent with the physiological stress associated with altered environmental conditions during transfer from field to laboratory, xenobiotic exposure, and nanoparticle toxicity. The enhanced protein inhibition in AgNP-treated samples corroborates reports of species-specific cytotoxicity of silver nanoparticles toward cyanobacteria and microalgae (Dulman et al., 2020; Seelam et al., 2017, 2018). Mechanistically, this may involve disruption of cellular membrane integrity, interference with enzymatic function, and oxidative stress generated by Ag^+ ion release from nanoparticle surfaces. The Acid Red dye similarly reduced protein content, consistent with the documented inhibitory effects of azo dye chromophores and their reductive metabolites on microbial enzyme systems (Tasi-Lu & Liu, 2001; Mohd & Ansari, 2015).

The synergistic protein inhibition in the combined dye + AgNP treatment is particularly noteworthy. This interaction may be attributed to: (i) dye sensitization of AgNP surfaces, generating ROS under ambient light conditions through a heterogeneous photocatalytic mechanism; (ii) dye-mediated disruption of the biogenic capping layer, accelerating Ag^+ ion release; or (iii) concurrent impairment of multiple metabolic pathways, overwhelming cellular antioxidant defense systems. Analogous synergistic effects have been reported for AgNP + dye systems in previous studies (Jyoti & Ajeet, 2016; Modi et al., 2015), lending support to this interpretation. From a remediation standpoint, this synergism is beneficial—enhancing dye transformation efficiency—but the concurrent amplification of biological stress demands careful dosage calibration before environmental application.

The statistical non-significance of inter-group differences at $\alpha = 0.05$, despite the clearly observable biological trends, reflects the fundamental challenge of small-sample ecotoxicological studies. The strong negative temporal correlations ($r = -0.95$ to -0.99) validate the biological patterns and suggest that extended incubation periods, larger sample replication, and a broader range of nanoparticle concentrations would likely achieve statistical significance. Future investigations should incorporate sub-lethal chronic exposure designs, species-level community profiling, and multi-endpoint toxicity batteries (including chlorophyll fluorescence, ROS quantification, and membrane integrity assays) to comprehensively characterize the ecological impact of pond water-derived AgNPs.

Collectively, this study establishes proof-of-concept for the utilization of natural pond water as a sustainable, zero-cost bioreductive medium for AgNP synthesis and demonstrates measurable dye-degradation activity. However, the ecotoxicological caution flag raised by protein suppression data underscores the dual-edged nature of nano-bioremediation: the same properties that confer pollutant degradation efficiency—high surface reactivity, ROS generation, and membrane interaction—also render AgNPs potentially hazardous to non-target aquatic organisms. Regulatory frameworks and life-cycle assessments must, therefore, accompany technological development to ensure that green nanotechnology does not introduce new ecological burdens in attempting to resolve existing ones (Kaul & Sharma, 2022; Bundschuh, 2016).

Conclusions

The present study successfully demonstrated the one-pot biogenic synthesis of silver nanoparticles using natural pond water as an ecologically sourced reducing and stabilizing medium. XRD analysis confirmed formation of crystalline fcc metallic silver with (111) preferential orientation; FE-SEM revealed predominantly spherical particles (150–300 nm); and EDX verified elemental silver composition with biogenic surface residues. Applied against Acid Red dye in a semi-natural aquatic system, the biosynthesized AgNPs produced a measurable decline in microbial protein content, with the combined AgNP + Dye treatment exhibiting the greatest inhibition—indicative of synergistic dye transformation and biological stress. Statistical correlations confirmed a consistent, progressive metabolic suppression trend across all treatments. These results establish the dual capacity of pond water-derived AgNPs as eco-friendly nano-bioremediation agents and potential ecotoxicants, reinforcing the imperative for rigorous dosage optimization, ecological risk assessment, and long-term environmental monitoring as prerequisites for scalable application in dye-contaminated wastewater management.

Acknowledgements

The authors gratefully acknowledge the scientific guidance of Dr. Manoj Kumar in the conceptualization and critical review of this manuscript. Sincere thanks are due to Mr. Dinesh Jaiswal, Central Instrumentation Laboratory (CIL), Banaras Hindu University, for instrumental support during XRD and FE-SEM characterization. The authors also appreciate the technical assistance of Mr. Santosh Jee, Mr. Dinesh Jee, and Mr. Akhilesh Jee during experimental execution. The institutional facilities and support provided by Shri A.K. Post Graduate College, Varanasi, are

gratefully acknowledged.

Conflict of Interest: The authors declare no conflict of interest.

References

1. Ahmad, N., Sharma, S., Singh, V. N., Shamsi, S. F., Fatma, A., & Mehta, B. R. (2010). Biosynthesis of silver nanoparticles from Desmodium triflorum: A novel approach towards weed utilization.
2. Biotechnology Research International, 2011, Article 454090.
3. Bundschuh, M. (2016). Ecotoxicological aspects of nanomaterials. Aquatic Toxicology, 170, 1–8.
4. Chugh, D., Kumar, A., Kumar, R., & Kumar, V. (2021). Green synthesis of silver nanoparticles and their applications: A review. Environmental Nanotechnology, Monitoring & Management, 15, 100431.
5. https://doi.org/10.1016/j.enmm.2021.100431
6. Crini, G., & Lichtfouse, E. (2019). Advantages and disadvantages of techniques used for wastewater treatment. Environmental Chemistry Letters, 17, 145–155.
7. Cristafulli-Bunsu, A. (2016). Nanoparticle toxicity in aquatic organisms. Toxicological Sciences, 153(2), 214–226.
8. Dahnormane, S., Ahmed, T., & Khan, M. (2017). Biosynthesis of silver nanoparticles and their role in dye degradation. Materials Letters, 209, 306–310.
9. Dedman, C. J., Newson, T. A., & Lead, J. R. (2015). Aquatic toxicity of silver nanoparticles in algae: A critical review. Science of the Total Environment, 530–531, 81–93.
10. Dulman, C. T., Popa, L., & Ivan, A. (2020). Silver nanoparticle effects on cyanobacterial biomass and protein content. Ecotoxicology and Environmental Safety, 192, 110312.
11. Fu, F., & Wang, Q. (2011). Removal of heavy metal ions from wastewater: A review. Journal of Environmental Management, 92(3), 407–418.
12. Granbardella, C., Bebianno, M. J., & Gomes, T. (2015). Effects of silver nanoparticles on marine phytoplankton. Marine Environmental Research, 111, 51–59.
13. Gupta, S., & Singhal, R. (2020). Advanced oxidation processes for wastewater treatment. Water Environment Research, 92(10), 1482–1495.
14. Huang, Y., Chen, Q., Deng, M., Japenga, J., & Li, T. (2016). Toxicological effects of silver nanoparticles on aquatic algae. Chemosphere, 152, 200–208.
15. Iravani, S. (2011). Green synthesis of metal nanoparticles using plants. Green Chemistry, 13, 2638–2650.
16. Jemal Kero, J., Alemayehu, M., & Desta, A. (2017). Algae-mediated biosynthesis of silver nanoparticles: Characterization and application in dye degradation. Journal of Nanomaterials, 2017, 4212956.
17. Jyoti, K., & Ajeet, P. (2016). Green synthesis of silver nanoparticles and their synergistic effect in dye degradation. Applied Nanoscience, 6, 223–230.
18. Kaul, R., & Sharma, P. (2022). Nanobioremediation: Principles, perspectives, and prospects.
19. Environmental Research, 209, 112805.
20. Modi, S., Kumar, R., & Ranjan, R. (2015). Nanoparticle-assisted dye degradation in aquatic systems.
21. Journal of Environmental Science and Health, Part A, 50(12), 1180–1190.
22. Mohd, K. I. A., & Ansari, F. A. (2015). Tolerance of cyanobacteria to methyl red dye. International Journal of Environmental Science and Technology, 12(8), 2643–2652.
23. Nithya, R., Sudha, S., & Ramasamy, P. (2019). Decolorization of Congo red by silver nanoparticles synthesized using Aspergillus niger broth. Environmental Nanotechnology, Monitoring & Management, 12, 100244.
24. Pal, S., Tak, Y. K., & Song, J. M. (2007). Does the antibacterial activity of silver nanoparticles depend on the shape of the nanoparticle? Applied and Environmental Microbiology, 73(6), 1712–1720.
25. Qu, X., Alvarez, P. J., & Li, Q. (2013). Applications of nanotechnology in water and wastewater treatment. Water Research, 47(12), 3931–3946.
26. Rai, M., Yadav, A., & Gade, A. (2012). Silver nanoparticles as a new generation of antimicrobials.
27. Biotechnology Advances, 27(1), 76–83.
28. Rathodur, A. K. (2021). Advances in nanobioremediation: Applications in wastewater treatment. Journal of Environmental Management, 294, 113030.
29. Rehman, F. (2020). Environmental implications of untreated wastewater discharge. Journal of Environmental Science and Health, 55(3), 289–298.
30. Sarkar, R., Kundu, S., & Ghosh, S. (2010). Biosynthesis of silver nanoparticles using algae and their application in dye degradation. Journal of Nanoscience and Nanotechnology, 10(1), 1–5.
31. Seelam, M., Kumar, V., & Sharma, P. (2017). Toxic effects of silver nanoparticles on green algae Chlamydomonas sp. Aquatic Toxicology, 189, 1–11.
32. Seelam, M., Sharma, P., & Kumar, A. (2018). Comparative ecotoxicity of silver nanoparticles in marine microalgae. Ecotoxicology, 27(4), 511–522.
33. Song, J. Y., & Kim, B. S. (2009). Rapid biological synthesis of silver nanoparticles using plant leaf extracts. Bioprocess and Biosystems Engineering, 32(1), 79–84.
34. Tasi-Lu, H., & Liu, S. (2001). Toxicity and biodegradation of azo dye Acid Red by activated sludge.

35. Water Research, 35(1), 291–298.
36. Veronica, R., Shalini, P., & Kumar, D. (2023). Dual-functional silver nanoparticles: Antimicrobial and photocatalytic dye degradation potential. Environmental Technology & Innovation, 30, 103053.
37. Vidali, M. (2001). Bioremediation: An overview. Pure and Applied Chemistry, 73(7), 1163–1172.